Supplementary File

Sea Surface Temperature over the Bay of Bengal: A key driver for South Asian Summer Monsoon rainfall during past 31 kiloyears

Thamizharasan Sakthivel [1,2], Prosenjit Ghosh[1,2] *, Ravi Bhushan[3], Harsh Raj[3], Ankur J Dabhi[3], Ajay Shivam[3], Senthilnathan D[4]

[1]Centre for Earth Sciences, Indian Institute of Science, Bangalore, India 560012.

[2]Divecha Centre for Climate Change, Indian Institute of Science, Bangalore, India 560012.

[3]Geosciences Division, Physical Research Laboratory, Ahmedabad, India 380009.

[4]Department of Earth Sciences, Pondicherry University, Puducherry, India 605014.

Correspondence to: Prosenjit Ghosh (pghosh@iisc.ac.in)

This PDF file includes:

Supplementary text

Fig. S1 to S6

Title for supplementary table

Other Supplementary Materials for this manuscript include the following:

Date S1 to S5

Supplementary text:

Error propagation for ΔSSS estimates:

The relationship between SSS and $\delta^{18}O_{sw}$ is expressed using Rayleigh steady model as follows:

$$\frac{SSS}{S_0} = \left[\frac{\delta^{18}O_{sw} \times (1-\beta)}{(\beta \times \delta^{18}O_{freshwater}) - \varepsilon_{vap/liq})}\right] + 1 \rightarrow (1)$$

For error propagation, we only considered the error associated with $\delta^{18}O_{sw}$ and didn't take into account the errors associated with other variables such as ß, $\varepsilon_{vap/liq}$, and $\delta^{18}O_{freshwater}$.

To simplify the mathematical error propagation process, we assigned letter to each variable, where

$A = 1 - \beta \rightarrow (2)$

$B = \varepsilon_{vap/liq} \rightarrow (3)$

$C = \beta \times \delta^{18}O_{freshwater} \rightarrow (4)$

$D = \delta^{18}O_{sw} \rightarrow (5)$

$E = S_0 \rightarrow (6)$

The substitution of (2, 3, 4, 5, and 6) into equation (1) becomes:

$$SSS = \left[\frac{D \times A \times E}{C - B}\right] + E \rightarrow (7)$$

The formula for error propagation is:

$$\delta SSS = \sqrt{\left(\frac{\partial SSS}{\partial A} \times \delta A\right)^2 + \left(\frac{\partial SSS}{\partial B} \times \delta B\right)^2 + \left(\frac{\partial SSS}{\partial C} \times \delta C\right)^2 + \left(\frac{\partial SSS}{\partial D} \times \delta D\right)^2 + \left(\frac{\partial SSS}{\partial E} \times \delta E\right)^2} \rightarrow (8)$$

Given that A, B, C, and E are constant, their respective error terms are (δA, δB, δC, and δE) zero, hence:

$$\delta\text{SSS} = \sqrt{\left(\frac{\partial\text{SSS}}{\partial\text{D}} \times \delta\text{D}\right)^2} \rightarrow (9)$$

The partial derivative of SSS with respect to the D variable is:

$$\frac{\partial\text{SSS}}{\partial\text{D}} = \frac{\text{AE}}{(\text{C}-\text{B})} \rightarrow (10)$$

$$\delta\text{SSS} = \sqrt{\left(\frac{\text{AE}}{(\text{C}-\text{E})} \times \delta\text{D}\right)^2} = \left|\frac{\text{AE}}{(\text{C}-\text{E})}\right| \times \delta\text{D} \rightarrow (10)$$

Supplementary Figures:

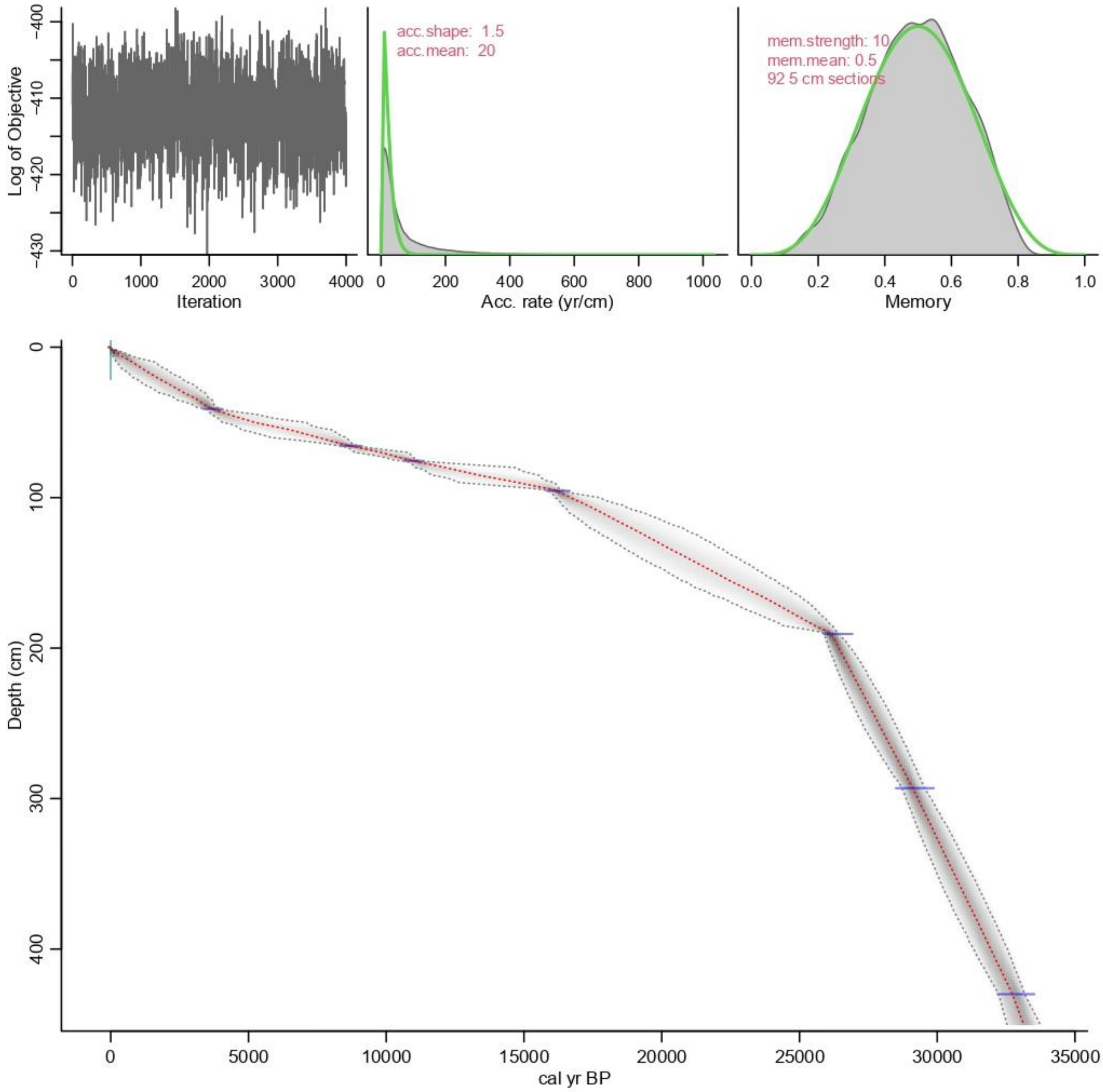

Fig S1: Age-Depth Model for Sediment Core MGS17/GC02. The Bacon age-depth model (Blaauw and Christen, 2011) for the sediment core from CWBoB is constructed using 7 radiocarbon ages obtained from mixed planktonic foraminifera species *G. ruber* and *G. sacculifer*. The core top is assumed to represent the present day. The gray dotted lines indicate the 95% confidence intervals, while the red dotted line represents the best fit ages, determined by the weighted mean age for each depth interval. The radiocarbon data and Bacon model output are provided in Table S1.

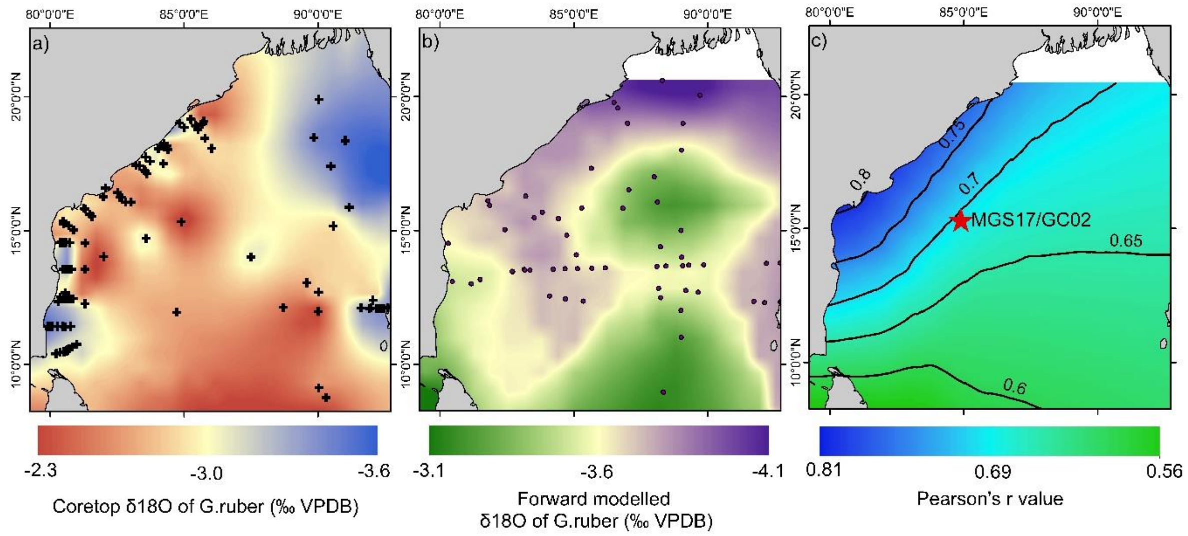

Fig. S2: Comparison between core-top δ^{18}O values of *G. ruber* and forward-modeled based estimates of δ^{18}O in *G. ruber*: a) Spatial mapping of core-top (0-1 cm; locations highlighted with a plus symbol) δ^{18}O values in *G.ruber* (refer to Table S4) interpolated by using the kriging interpolation method; b) For forward modelling, δ^{18}O in seawater from the BoB region are collated (refer to Table S2; locations highlighted with purple dots), together with the average SST data from MERRA-2 reanalysis (1980-2023) (Global Modeling and Assimilation Office, n.d.) during the South Asian Summer Monsoon (SASM) period (June to September) is used for deducing the carbonate d18O values. These SST and δ^{18}O seawater values are input parameters for the estimation of δ^{18}O values in *G. ruber* (Mulitza et al., 2003) at equilibrium and interpolated using the Kriging interpolation technique. c) A geographically weighted regression method (Mitchell, 2005) is used for the estimation of Pearson's correlation coefficient (r-value) between observed core-top δ^{18}O values in G. ruber and predicted δ^{18}O values in *G. ruber* using a forward-modelling approach.

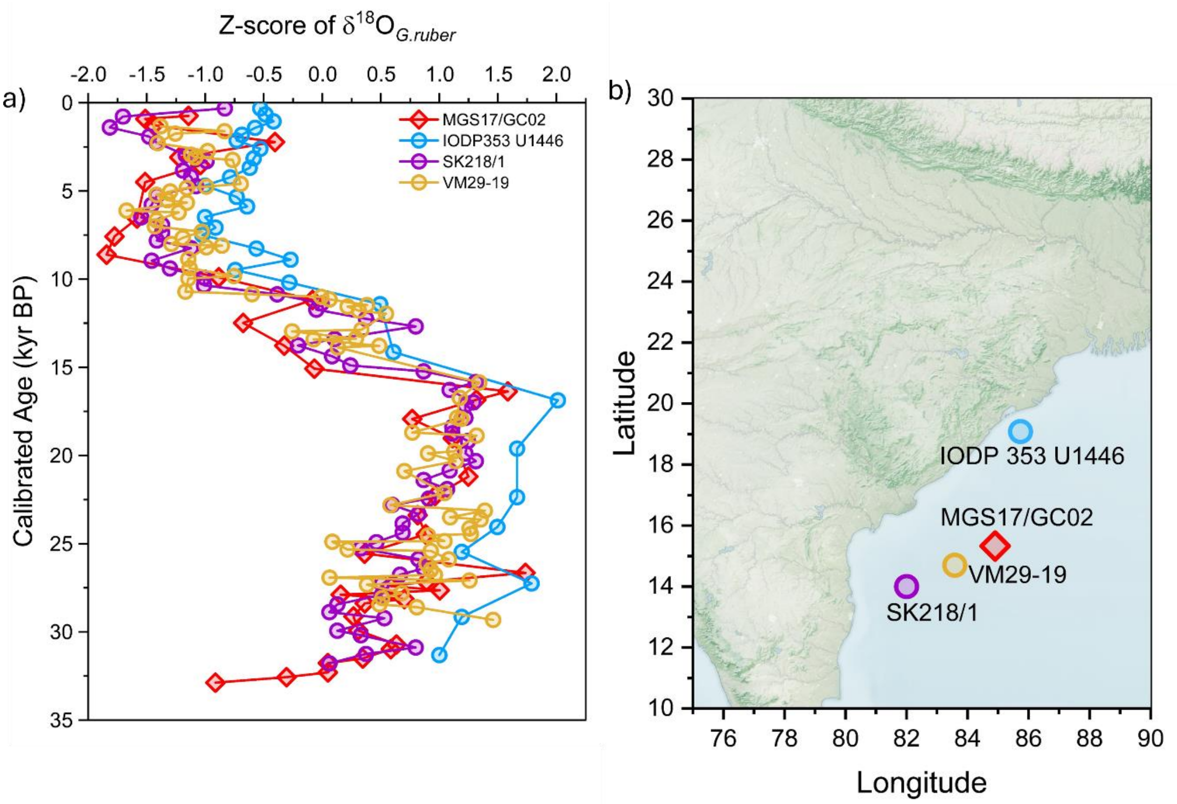

Fig. S3: Spatio-temporal comparison of δ^{18}O variability in *G. ruber* across sites over BoB. a) Time series comparison of Z-scores of δ^{18}O in *G. ruber* from the present study site (MGS17/GC02) with available records from adjacent sites VM29-19(Rashid et al., 2011), SK218/1(Govil and Divakar Naidu, 2011), and IODP Expedition 353 Site U1446(Clemens et al., 2021). b) Panel displaying the locations of these sites. The pattern observed shows the regional heterogeneity in sea surface temperature and salinity which governs the δ^{18}O measured in shell carbonate.

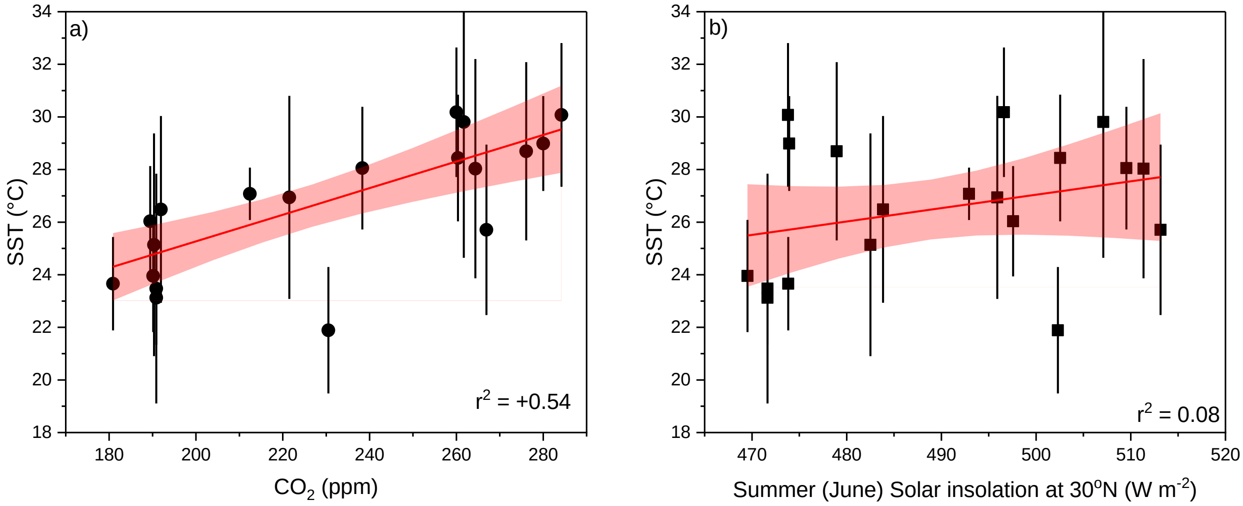

Fig. S4: Sensitivity analysis of estimated SST (1.6 kyr resolution) with climate forcing (a) mean atmospheric CO_2 record from Antarctic ice core (Bereiter et al., 2015) and (b) expected mean summer (June) time solar insolation at 30°N (Berger, 1992), during past 31 kiloyears BP.

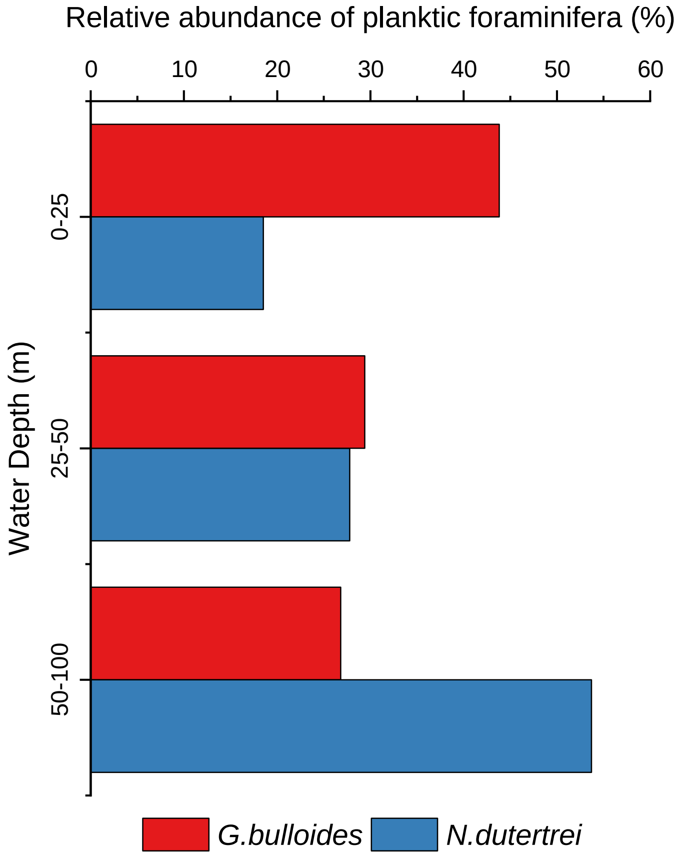

Fig. S5: Depth-wise preferred habitat of *G. bulloides* and *N. dutertrei* in sites over Northern Indian Ocean. The relative abundance is based on plankton net samples collected at depths of 0-25m, 25-50m, and 50-100m in the coastal waters of Sumatra (Latitude: 1°N to 6°S; Longitude: 96°E to 103°E) (Tapia et al., 2022). Here, we presented data for a 100m water depth.

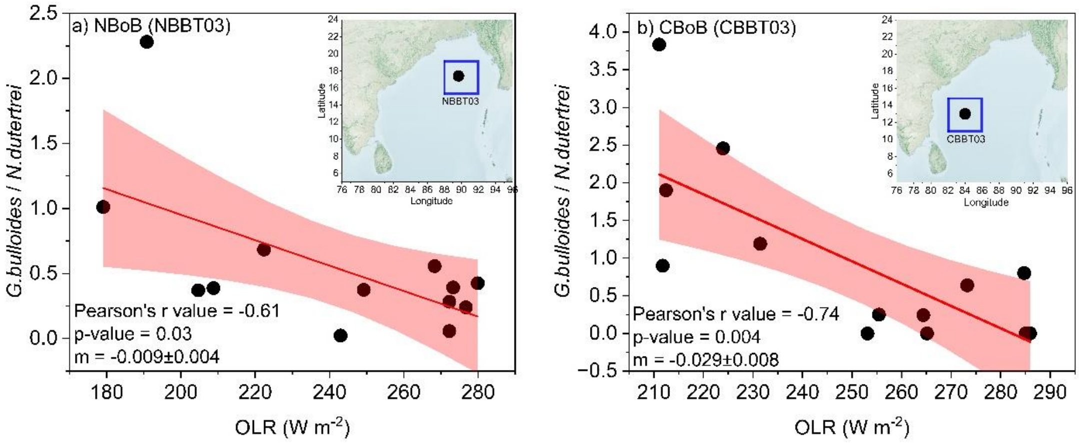

Fig. S6: Relationship between the *G. bulloides* to *N. dutertrei* ratio and cloud cover index deduced from Outgoing Longwave Radiation (OLR) over the BoB. (a) We presented sediment trap data from NBBT03, located in the NBoB, which was programmed to collect 13 successive samples, each spanning a duration of 27 days, between November 16, 1988, and October 6, 1989. Planktic foraminiferal counts were conducted on samples collected at 2 depths, 967m and 1498m, with a size fraction ranging between 150µm to 500µm(Guptha et al., 1997). (b) Sediment trap CBBT03 was deployed over the region CWBoB, which was operational and coinciding with NBBT03. Planktic foraminiferal counts were conducted on samples collected from one depth at 950m(Guptha et al., 1997). Interpolated monthly OLR values were obtained for both sites for the period of observations at NBBT03 and CBBT03, and a 4°x4° grid was designed with each site as the focal point (Liebmann and Smith, 1996).

Title for the supplementary table:

Table S1: Radiocarbon Data and Bacon Age-Model Output

Table S2: $\delta^{18}O$ of seawater record over the Bay of Bengal during SASM (JJAS).

Table S3: Estimation of $\delta^{18}O$ of freshwater input to the Bay of Bengal.

Table S4: Raw Values and Corrections for clumped and stable isotope analysis, Temperature estimation, stable oxygen isotope of seawater estimation, and error propagation.

Table S5: Calculation of ΔSSS between NBoB and CWBoB.

Reference:

Bereiter, B., Eggleston, S., Schmitt, J., Nehrbass-Ahles, C., Stocker, T.F., Fischer, H., Kipfstuhl, S., Chappellaz, J., 2015. Revision of the EPICA Dome C CO2 record from 800 to 600-kyr before present. Geophys. Res. Lett. 42, 542–549. https://doi.org/10.1002/2014GL061957

Berger, A., 1992. Orbital Variations and Insolation Database. NOAA/NGDC Paleoclimatology Program, Boulder CO, USA.

Blaauw, M., Christen, J.A., 2011. Flexible paleoclimate age-depth models using an autoregressive gamma process. Bayesian Anal. 6, 457–474. https://doi.org/10.1214/11-ba618

Clemens, S.C., Yamamoto, M., Thirumalai, K., Giosan, L., Richey, J.N., Nilsson-Kerr, K., Rosenthal, Y., Anand, P., McGrath, S.M., 2021. Remote and local drivers of pleistocene South Asian summer monsoon precipitation: A test for future predictions. Sci. Adv. 7, 1–16. https://doi.org/10.1126/sciadv.abg3848

Global Modeling and Assimilation Office, n.d. MERRA-2 tavgM_2d_ocn_Nx: 2d,Monthly mean,Time-Averaged,Single-Level,Assimilation,Ocean Surface Diagnostics V5.12.4, Greenbelt, MD, USA, Goddard Earth Sciences Data and Information Services Center (GES DISC), Accessed:27/04/2024. https://doi.org/https://doi.org/10.5067/4IASLIDL8EEC

Govil, P., Divakar Naidu, P., 2011. Variations of Indian monsoon precipitation during the last 32kyr reflected in the surface hydrography of the Western Bay of Bengal. Quat. Sci. Rev. 30, 3871–3879. https://doi.org/10.1016/j.quascirev.2011.10.004

Guptha, M.V.S., Curry, W.B., Ittekkot, V., Muralinath, A.S., 1997. Seasonal variation in the flux of planktic Foraminifera; sediment trap results from the Bay of Bengal, northern

Indian Ocean. J. Foraminifer. Res. https://doi.org/10.2113/gsjfr.27.1.5

Liebmann, Smith, 1996. NOAA Interpolated Outgoing Longwave Radiation (OLR) data provided by the NOAA PSL, Boulder, Colorado, USA, from their website at https://psl.noaa.gov. Bull. Am. Meteorol. 77, 1275–1277.

Mitchell, A., 2005. The ESRI Guide to GIS Analysis. Volume 2. ESRI press.

Mulitza, S., Boltovskoy, D., Donner, B., Meggers, H., Paul, A., Wefer, G., 2003. Temperature: δ18O relationships of planktonic foraminifera collected from surface waters. Palaeogeogr. Palaeoclimatol. Palaeoecol. https://doi.org/10.1016/S0031-0182(03)00633-3

Rashid, H., England, E., Thompson, L., Polyak, L., 2011. Late glacial to holocene indian summer monsoon variability based upon sediment records taken from the bay of Bengal. Terr. Atmos. Ocean. Sci. https://doi.org/10.3319/TAO.2010.09.17.02(TibXS)

Tapia, R., Ho, S.L., Wang, H.Y., Groeneveld, J., Mohtadi, M., 2022. Contrasting vertical distributions of recent planktic foraminifera off Indonesia during the southeast monsoon: implications for paleoceanographic reconstructions. Biogeosciences 19, 3185–3208. https://doi.org/10.5194/bg-19-3185-2022